# Resonant Coupling of Landau Levels via LO Phonons in Polar Semiconductors and its Effects on the Landau-Level Raman Scattering from Semiconductor Plasmas*

K. L. Ngai

*Lincoln Laboratory, Massachusetts Institute of Technology, Lexington, Massachusetts* 02173

(Received 17 August 1970)

The Green's -function method for studying the resonant coupling of Landau levels via LO phonons is reexamined, and the approximations made therein are justified. The coupling between the $n=2$ Landau level and the $n=1$ Landau level plus one-LO-phonon continuum is investigated under the condition that the cyclotron frequency $\omega_c$ is nearly equal to the LO-phonon frequency $\omega_0$. Since the $n=1$ Landau level has been resonantly coupled to the $n=0$ Landau level plus one-LO-phonon continuum under the same condition, novel features of the electron energy spectrum appear. It is shown that the pinning effect that occurs for the $n=1$ Landau level exists also for the $n=2$ level. The cross section for the inelastic light scattering from electron plasmas in polar semiconductors under the influence of a dc magnetic field is calculated approximately with the inclusion of electron-phonon polar interaction. The effect of both Coulomb interactions and electron-phonon interactions on the momentum matrix elements occurring in the calculation is neglected, but is kept in the evaluation of the correlation function of a generalized pair operator. The results of scattering from single-particle excitations between the $n=0$ and $n=2$ Landau levels exhibits the effect of the resonant coupling between the $n=2$ and $n=1$ levels via LO phonons. However, for scattering from collective modes such as the coupled LO-phonon–magnetoplasma mode and the Bernstein modes, the possibility of observing similar resonant coupling effects is ruled out.

## I. INTRODUCTION

An electron in a polar lattice will always carry with it a lattice polarization field. The composite particle, electron plus phonon field, is called the polaron. In the presence of a magnetic field, of sufficient strength that the cyclotron energy $\omega_c$ is near the energy of a LO phonon $\omega_0$, polaron self-energy effects are expected to be strongly enhanced. The magnetic field is chosen to be in the $z$ direction and described by a vector potential in the Landau gauge $\vec{A}_0=(0, Hx, 0)$. The single-particle states in the Landau representation can be described by a set of quantum numbers $\alpha\equiv\{n, k_y, k_z\}$ and an energy

$$\epsilon_\alpha^0=(n+\tfrac{1}{2})\hbar\omega_c+\hbar^2k_z^2/2m^* \quad .$$

Then under the condition $\omega_c\approx\omega_0$, the state of an $\{n=1, k_y, k_z\}$ electron with energy $\frac{3}{2}\hbar\omega_c+\hbar^2k_z^2/2m^*$ is nearly degenerate with a continuum of states consisting of an $\{n=0, k_y-q_y, k_z-q_z\}$ electron plus one phonon of wave vector $\vec{q}$ with energy

$$\tfrac{1}{2}\hbar\omega_c+\hbar^2(k_z-q_z)^2/2m^*+\hbar\omega_0 \quad .$$

The electron-phonon (el-ph) coupling causes a strong mixing of these states,[1,2] and since the density of states of the continuum has a singularity $(E-E_c)^{-1/2}$ at $E_c=\frac{1}{2}\hbar\omega_c+\hbar\omega_0$, the resonant enhancement of the polaron effects is apparent. This resonant coupling of Landau levels in polar semiconductors such as InSb has been observed by magneto-optical methods such as interband magnetoabsorption,[1,2] impurity absorption,[3,4] cyclotron resonance,[5–8] and combined resonance.[9] These experiments have revealed the energy spectrum of the el-ph system. Recent advances in the development of inelastic light scattering as an effective tool for studying the excitation spectrum of electron carriers in semiconductor crystals leads one naturally to ask the question of how the resonant coupling of Landau levels manifests itself in light-scattering experiments. The object of this paper is to answer this question. Various theoretical calculations of light-scattering cross sections from excitations in semiconductor magnetoplasmas have been given.[10–17] We shall in particular adopt a recent approach by Blum[17] who has extended the treatment of Hamilton and McWhorter[13] to magnetoplasma light scattering. The el-ph interaction (EPI) shall be incorporated into Blum's treatment and effects due to resonant coupling are derived. In the course of the discussion we shall clarify and justify several approximations often made in calculating the polaron self-energy effects in resonant coupling. For example, the vertex corrections are shown to be unimportant, i.e., the corrections to the free vertex are smaller by a factor of $\alpha_0/|(E-E_c)/\hbar\omega_0|^{1/2}$, where $\alpha_0$ is the Fröhlich constant.

We begin by deriving a general expression for the inelastic scattering cross section of light by a semiconductor magentoplasma with inclusion of el-ph

interaction. In Sec. III we shall study the el-ph coupling of Landau levels. The general discussions therein are applied to the special case of the $n=2$ Landau level. Interesting novel features of its level scheme and its manifestation in the Landau-Raman scattering spectrum constitutes Sec. V.

## II. CROSS SECTION FOR INELASTIC SCATTERING OF LIGHT

In this section we shall follow the approach of Hamilton and McWhorter and of Blum to derive a general expression for the cross section for the inelastic scattering of light by a semiconductor magnetoplasma with inclusion of EPI. For ease of comparison with and reference to Blum, we shall adopt his notation as much as possible. The Hamiltonian of the electron system in a crystalline polar lattice is

$$\mathcal{H}=\sum_{\alpha}\epsilon_{\alpha}c_{\alpha}^{\dagger}c_{\alpha}+\sum_{\alpha,\beta,\vec{Q}}[\upsilon_{\beta\alpha}(\vec{Q})b_{\vec{Q}}+\upsilon_{\beta\alpha}^{*}(\vec{Q})b_{\vec{Q}}^{\dagger}]c_{\beta}^{\dagger}c_{\alpha}+\tfrac{1}{2}\sum_{\vec{q}}v(\vec{q})\sum_{\alpha\beta\gamma\delta}m_{\alpha\beta}m_{\gamma\delta}^{*}\,c_{\alpha}^{\dagger}c_{\gamma}^{\dagger}c_{\delta}c_{\beta}+\sum_{\vec{Q}}\hbar\omega_{0}b_{\vec{Q}}^{\dagger}b_{\vec{Q}}\ , \tag{1}$$

where $v(\vec{q})=4\pi e^{2}/q^{2}\epsilon_{\infty}$, $m_{\alpha\beta}=\langle\alpha|e^{i\vec{q}\cdot\vec{r}}|\beta\rangle$, $c_{\alpha}^{\dagger}$ and $c_{\alpha}$ are the creation and annihilation operators for the single-particle eigenstates $|\alpha\rangle$. The latter satisfy $\mathcal{H}_{0}|\alpha\rangle=\epsilon_{\alpha}^{0}|\alpha\rangle$ with

$$\mathcal{H}_{0}=\frac{[\vec{p}-(e/c)\vec{A}_{0}]^{2}}{2m}+V(\vec{r})+\frac{\hbar[\vec{p}-(e/c)\vec{A}_{0}]\cdot(\vec{\sigma}\times\vec{\nabla}V)}{4m^{2}c^{2}}+\tfrac{1}{2}g\mu_{B}\vec{\sigma}\cdot\vec{B}_{0} \tag{2}$$

as the Hamiltonian of an electron in the crystalline lattice in the presence of a static uniform magnetic field. The crystal periodic potential and the spin-orbit coupling term have been included. In (1), $\upsilon_{\beta\alpha}(Q)\equiv\langle\beta|\upsilon(Q)|\alpha\rangle$ is the Fröhlich interaction[18] defined in detail later in (17a). As has been emphasized by Blum, the form of $\mathcal{H}_{0}$ in (2) has the advantage over the treatments which replace $\mathcal{H}_{0}$ by an effective one-band Hamiltonian because resonant enhancement effects and one-electron effects, such as nonparabolicity and spin-orbit coupling are included automatically. In the presence of an electromagnetic radiation field represented by a vector potential $\vec{A}_{\omega}(\vec{r})$ we replace the momentum $\vec{p}$ in (2) by $[\vec{p}-(e/c)\vec{A}_{\omega}]$ to approximate the electron-to-light coupling. Treating $\vec{A}_{\omega}$ as a perturbation, the differential cross section for scattering of a photon from state $(\omega_{I},\vec{k}_{I},\hat{\epsilon}_{I})$ to state $(\omega_{F},\vec{k}_{F},\hat{\epsilon}_{F})$, while the electronic system has undergone a transition from a many-electron initial state $|I\rangle$ to state $|F\rangle$ is[13]

$$\frac{d^{2}\sigma}{d\omega\,d\Omega}=\hbar\frac{\omega_{F}}{\omega_{I}}\langle\textstyle\sum|M_{FI}|^{2}\delta(E_{F}-E_{I}-\hbar\omega)\rangle\ , \tag{3}$$

where $\omega=\omega_{I}-\omega_{F}$ and the angular brackets denote a statistical average over the initial states. We are interested here in scattering processes such that the initial and final electron states $|I\rangle$ and $|F\rangle$ differ only by excitation of electrons within the conduction band of the semiconductor; then we have[17]

$$M_{FI}=\sum_{\alpha\beta}\gamma_{\alpha\beta}\langle F|c_{\alpha}^{\dagger}c_{\beta}|I\rangle\ , \tag{4}$$

where

$$\gamma_{\alpha\beta}=\frac{e^{2}}{mc^{2}}\left[m_{\alpha\beta}\hat{\epsilon}_{I}\cdot\hat{\epsilon}_{F}+\frac{1}{m}\sum_{\beta'}\left(\frac{\langle\alpha|j_{F}|\beta'\rangle\langle\beta'|j_{I}|\beta\rangle}{E_{\beta}-E_{\beta'}+\hbar\omega_{I}}+\frac{\langle\alpha|j_{I}|\beta'\rangle\langle\beta'|j_{F}|\beta\rangle}{E_{\alpha}-B_{\beta'}-\hbar\omega_{I}}\right)\right]\ . \tag{5}$$

In arriving at this approximate form for $M_{FI}$ we have neglected the effect of both the Coulomb interaction and the el-ph interactions on the momentum matrix elements and the energy denominators appearing in (5).

This neglect of the effect of el-ph polar coupling on $\gamma_{\alpha\beta}$ is justified through a calculation by Harper[19] of the polaron-induced scattering cross section. It has been pointed out by Wolff[11] that unperturbed Landau states of free electrons behave as pure harmonic oscillators and cannot scatter in the dipole approximation. Harper[19] noticed that an effect of the polaron coupling on the Landau levels is to provide a source of anharmonicity that can induce scattering. Using a different formulation of light scattering from ours, Harper essentially evaluated the modifications of the *intraband* intermediate-state contributions to $\gamma$ due to polar coupling to phonons, and was led to the result that the polaron-interaction-induced contribution to the scattering cross section $\sigma_{2\omega_{c}}$ per particle is of $O(\alpha_{0}^{2}\sigma_{T}^{*})$, where $\sigma_{T}^{*}=e^{2}/m^{*}c^{2}$ is the effective Thomson cross section. The estimate is given for the case in which the magnetic field is strong enough when only the $n=0$ Landau level is occupied and electron transition is from $n=0$ to $n=2$ in the Landau-Raman scattering process. Nevertheless, in scattering from a conduction-band plasma the only important contribution to $\gamma$ is from *interband* intermediate states, which leads to a cross section per particle for scattering parallel to the magnetic field ($q\|B_{0}$) given by $\sigma_{2\omega_{c}}=O[\sigma_{T}^{*}(\hbar\omega_{c}/E_{g})^{2}]$.[17] For InSb, $E_{g}\approx 237$ meV, $\alpha_{0}=0.02$, and if $\omega_{c}$ is nearly $\omega_{0}\approx 24$ meV, the LO-phonon energy, then Harper's polaron-interaction-induced contribution to scattering is roughly two orders of magnitude smaller than the interband contribution. This fact enables us to ignore el-ph–polar-coupling modifications on $\gamma_{\alpha\beta}$. Moreover,

the effect on the Landau-Raman scattering due to resonant coupling of Landau levels via LO phonons in polar semiconductors does not occur in the manner as Harper described it. With our present formulation of the problem we shall show how el-ph coupling enters the dominant interband contribution to scattering and induces magnetic-field-dependent structure in the scattered-light spectrum.

The electron-electron (el-el) and el-ph interactions will be kept in the evaluation of the matrix element of the generalized pair operator $c_\alpha^\dagger c_\beta$ and the correlation function of this operator as we shall discuss next.

From (4) the cross section can be expressed in terms of the Fourier transform of the correlation function $C(t)=\langle N^\dagger(t)N(0)\rangle$ for the generalized operator $N=\sum_{\alpha\beta}\gamma_{\alpha\beta}c_\alpha^\dagger c_\beta$,

$$\frac{d^2\sigma}{d\omega d\Omega}=\hbar\frac{\omega_F}{\omega_I}\int_{-\infty}^{\infty}\frac{dt}{2}\,e^{i\omega t}\langle N^\dagger(t)N(0)\rangle . \tag{6}$$

Often it is more convenient to work with corresponding retarded response function

$$R(t)=-i\theta(t)\langle[N^\dagger(t),N(0)]\rangle \ . \tag{7}$$

The Fourier transform of $C$ and $R$ are related by the fluctuation-dissipation theorem

$$C(\omega)=-2\mathrm{Im}[R(\omega)]/(1-e^{-\hbar\omega/k_BT}) \ . \tag{8}$$

Hence the light-scattering spectrum is

$$\frac{d^2\sigma}{d\omega d\Omega}=\hbar\frac{\omega_F}{\omega_I}\frac{1}{1-e^{-\hbar\omega/k_BT}}\,\mathrm{Im}[R(\omega)] \ . \tag{9}$$

From the definition of $R$ in (7) we have

$$R(t)=\sum_{\alpha\beta}\sum_{\delta\epsilon}\gamma_{\alpha\beta}^*\gamma_{\delta\epsilon}F_{\alpha\beta\delta\epsilon}(t) \tag{10}$$

and

$$F_{\alpha\beta\delta\epsilon}(t)=-i\theta(t)\langle[c_\beta^\dagger(t)c_\alpha(t),\ c_\delta^\dagger(0)c_\epsilon(0)]\rangle \ . \tag{11}$$

As is well known, nonzero temperature perturbation theory[20] is conveniently expressed in terms of Feynman graphs by methods of temperature-ordered thermodynamic Green's functions. The relevant thermal correlation function we shall introduce is

$$\mathcal{R}(\tau)=\sum_{\alpha\beta}\sum_{\delta\epsilon}\gamma_{\alpha\beta}^*\gamma_{\delta\epsilon}\mathcal{F}_{\alpha\beta\delta\epsilon}(\tau) \ , \tag{12}$$

where

$$\mathcal{F}_{\alpha\beta\delta\epsilon}(\tau)=-\langle T_\tau[c_\beta^\dagger(\tau)c_\alpha(\tau)c_\delta^\dagger(0)c_\epsilon(0)]\rangle \ . \tag{13}$$

Here $T_\tau$ is the time-ordering operator; $\tau$ ranges in the interval $(-1/k_BT,\ 1/k_BT)$, where $T$ is the absolute temperature. The "temporal" development of the operators is defined by

$$c_\alpha^\dagger(\tau)c_\beta(\tau)=e^{H\tau}c_\alpha^\dagger(0)c_\beta(0)e^{-H\tau} \ . \tag{14}$$

The Fourier transform of $\mathcal{F}_{\alpha\beta\delta\epsilon}(\tau)$ and $\mathcal{R}(\tau)$ ,

$$\mathcal{F}_{\alpha\beta\delta\epsilon}(i\omega_n)=\int_0^{1/k_BT}\mathcal{F}_{\alpha\beta\delta\epsilon}(\tau)e^{i\omega_n\tau}\,d\tau \ ,$$

$$\omega_n=2\pi nk_BT \tag{15}$$

in which $n$ is an integer, is related directly to the retarded response function via analytical continuation. That is, if $\mathcal{F}_{\alpha\beta\delta\epsilon}(z)\,[\mathcal{R}(z)]$ is obtained by analytical continuation of $\mathcal{F}_{\alpha\beta\delta\epsilon}(i\omega_n)[\mathcal{R}(i\omega_n)]$ from a discrete set of points into the entire upper half-plane, then $F_{\alpha\beta\delta\epsilon}(\omega)=\mathcal{F}_{\alpha\beta\delta\epsilon}(z\to\omega+i0)$ and $R(\omega)=\mathcal{R}(z\to\omega+i0)$. Thus our problem of light scattering reduces now to the evaluation of the thermal correlation function $\mathcal{F}_{\alpha\beta\delta\epsilon}(i\omega_n)$ or $\mathcal{R}(i\omega_n)$ by perturbation theory expressed in terms of Feynman graphs.[20] The perturbation is the sum of the Coulomb and el-ph interactions:

$$\mathcal{H}_I=\tfrac{1}{2}\sum_{\vec q}v(\vec q)\sum_{\alpha\beta\delta\epsilon}m_{\alpha\beta}m_{\delta\epsilon}^*c_\alpha^\dagger c_\delta^\dagger c_\epsilon c_\beta$$

$$+\sum_{\alpha\beta\vec Q}(v_{\beta\alpha}(\vec Q)b_{\vec Q}+v_{\beta\alpha}(\vec Q)b_{\vec Q}^\dagger)c_\beta^\dagger c_\alpha \ . \tag{16}$$

Effects due to both interactions will modify the electron excitation spectrum. However Coulomb effects are believed to be small.[21] Therefore, in Sec. III only the EPI contribution to the electron self-energy in the presence of a magnetic field is calculated. As is well known, EPI results in both renormalization and lifetime effects on an electron and can be fully described by the complex electron self-energy part $\Sigma_\alpha(\zeta_l)$ which shall be evaluated via the temperature diagram technique.[20] The associated exact electron propagator $G_\alpha(\zeta_l)$ is $1/[\zeta_l-\epsilon_\alpha^0-\Sigma_\alpha(\zeta_l)]$. In writing $\Sigma_\alpha$ and $G_\alpha$ as such, we have already used the fact that with inclusion of EPI only, both the electron self-energy part and the electron propagator are diagonal in the single-particle quantum numbers $\alpha$.[22] Detailed evaluation of $G_\alpha$ is relegated to Sec. III. With $G_\alpha$ at hand we shall calculate the correlation functions $\mathcal{F}_{\alpha\beta\delta\epsilon}(\omega+i0)$ or $\mathcal{R}(\omega+i0)$ in the presence of both Coulomb interaction and EPI.

## III. ELECTRON SPECTRUM

The Hamiltonian we start with is

$$\mathcal{H}=\sum_\alpha\epsilon_\alpha^0c_\alpha^\dagger c_\alpha+\sum_{\vec Q}\hbar\omega_{\vec Q}b_{\vec Q}^\dagger b_{\vec Q}$$

$$+\sum_{\alpha\beta\vec Q}[v_{\beta\alpha}(\vec Q)b_{\vec Q}+v_{\beta\alpha}^*(\vec Q)b_{\vec Q}^\dagger]c_\beta^\dagger c_\alpha \ . \tag{17a}$$

The Fröhlich Hamiltonian describes the el-ph system in a magnetic field

$$v_{\beta\alpha}(\vec Q)=-i\hbar\omega_0(4\pi\alpha_0/S)^{1/2}(1/Q)\langle\beta|e^{i\vec Q\cdot\vec r}|\alpha\rangle$$

$$\equiv v(\vec{Q}) m_{\beta\alpha} \quad . \tag{17b}$$

$S$ is the crystal volume in units of $r_0^3$, $r_0 = (\hbar/2m^*\omega_0)^{1/2}$, and

$$\alpha_0 = \frac{1}{2}\left(\frac{e^2}{r_0}\right)\left(\frac{1}{\hbar\omega_0}\right)\left(\frac{1}{\epsilon_\infty} - \frac{1}{\epsilon_0}\right)$$

is assumed to be $\ll 1$. The last term in (17a) is treated as a perturbation on eigenstates of the remainder of the Hamiltonian. It has been shown that the electron propagator of the Hamiltonian in (17a) is diagonal in the Landau representation.[22] That is, if

$$G_{\alpha\beta}(\zeta_l) = -\int_0^{1/k_BT} du\, e^{-\zeta_l u} \langle T c_\alpha(u) c_\beta^\dagger(0)\rangle \quad ,$$

with

$$\zeta_l = \mu + i(2l+1)\pi k_B T$$

and $\mu$ the chemical potential, then

$$G_{\alpha\beta}(\zeta_l) = \delta_{\alpha\beta} G_{\alpha\alpha}(\zeta_l) \quad .$$

Let $G_{\alpha\alpha}(\zeta_l) \equiv G_\alpha(\zeta_l)$, and

$$G_\alpha(\zeta_l) = [\zeta_l - \epsilon_\alpha^0 - \Sigma_\alpha(\zeta_l)]^{-1} \tag{18}$$

follows from Dyson's equation. The electron self-energy $\Sigma_\alpha(\zeta_l)$ is given as the diagram shown in Fig. 1. The shaded circle in Fig. 1 represents the full vertex part of EPI. Explicitly,

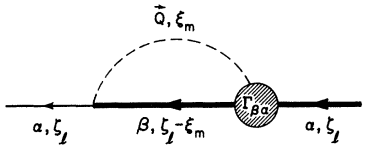


FIG. 1. Diagram for proper electron self-energy part.

$$\Sigma_\alpha(\zeta_l) = \frac{k_BT}{(2\pi)^3} \sum_{n_\beta, \xi_m} \int \frac{d\vec{Q}\, v^*_{\beta\alpha}(\vec{Q}) \Gamma_{\beta\alpha}(\vec{Q}, \zeta_l - \xi_m, \zeta_l)}{\zeta_l - \xi_m - \epsilon_\beta^0 - \Sigma_\beta(\zeta_l - \xi_m)} \times \frac{2\hbar\omega_Q}{\hbar^2\omega_Q^2 + \xi_m^2} \tag{19}$$

and $\xi_m = i2\pi m k_B T$.

To start with, let us first calculate the contribution to the electron proper self-energy part by the lowest-order skeleton diagram illustrated in Fig. 2. The evaluation of this diagram follows the basic method of replacing each electron or phonon line by the exact propagator [23]:

$$\Sigma_\alpha(\zeta_l) = \frac{k_BT}{(2\pi)^3} \sum_{n_\beta, \xi_m} d\vec{Q} |v_{\beta\alpha}(\vec{Q})|^2 \times \frac{1}{\zeta_l - \xi_m - \epsilon_\beta^0 - \Sigma_\beta(\zeta_l - \xi_m)} \frac{2\hbar\omega_Q}{\hbar^2\omega_Q^2 + \xi_m^2} \quad , \tag{20}$$

where $\omega_Q$ is the renormalized phonon frequencies. The summation over $\xi_m$ can be performed via standard techniques[22] with the result

$$\Sigma_\alpha(\zeta_l) = \frac{1}{2\pi i} \sum_{n_\beta, \vec{Q}} \int_{-\infty}^{\infty} dx\, |v_{\beta\alpha}(\vec{Q})|^2 \left(\frac{1}{x - \epsilon_\beta^0 - \Sigma_\beta(x - i0)} - \frac{1}{x - \epsilon_\beta^0 - \Sigma_\beta(x + i0)}\right)\left(\frac{1 - f(x) + N_Q}{\zeta_l - x - \hbar\omega_Q} + \frac{f(x) + N_Q}{\zeta_l - x + \hbar\omega_Q}\right), \tag{21}$$

where

$$N_Q = 1/(e^{\hbar\omega/k_BT} - 1)$$

and

$$f(x) = [1 + e^{(x-\mu)/k_BT}]^{-1} \quad .$$

The self-energy is discontinuous across the real axis in such a way that

$$\Sigma_\beta(x \pm i0) = \mathrm{Re}\Sigma_\beta(x) \mp i\, \mathrm{Im}\Sigma_\beta(x) \quad ,$$

and $\mathrm{Im}\Sigma_\beta(x) \geq 0$. Substitute this into (21) and analytically continue the $\Sigma_\alpha(\zeta_l)$ defined at isolated points in the complex plane to the real $\zeta$ axis, i.e., $\zeta \to E \pm i0$, and one obtains

$$\Sigma_\alpha(E \pm i0) = \sum_{n_\beta, \vec{Q}} \int_{-\infty}^{\infty} dx\, |v_{\beta\alpha}(\vec{Q})|^2 A_\beta(x) \times \left(\frac{1 - f(x) + N_q}{E - x - \hbar\omega_Q \pm i0} + \frac{f(x) + N_q}{E - x + \hbar\omega_Q \pm i0}\right) \quad . \tag{22}$$

We have introduced the spectral weight function $A_\beta(x)$ which is related to the thermal Green's function $G_\beta(x)$ as

$$A_\beta(x) = -1/\pi\, \mathrm{Im}G_\beta(x + i0) \quad . \tag{23}$$

After obtaining (22) for $\Sigma_\alpha(E \pm i0)$ we can first turn to the problem of the coupling between the $n = 1$ Landau level and the $n = 0$ level plus one LO phonon and make contact with the recent works by Korovin and Pavlov[24] and by Nakayama.[25] Under the condition that $\omega_c$ is nearly equal to $\omega_0$, we shall look for resonant coupling effects on the energy spectrum of an electron $|\alpha\rangle$ ($\equiv |n_\alpha, k_y, k_z\rangle$) in the $n_\alpha = 1$ state. Then only the $n_\beta = 0$ term in the sum over $n_\beta$ is re-

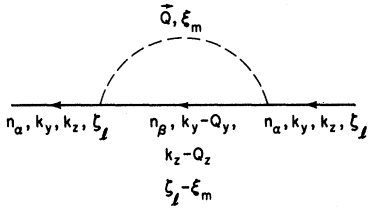


FIG. 2. Lowest-order skeleton diagram for the proper electron self-energy part.

tained because the rest are nonresonant contributions which we discard. In the energy range for resonance consideration an electron $|\beta\rangle$ in the $n_\beta = 0$ level cannot emit a LO phonon. $\Sigma_\beta$ is real, and

$$A_\beta(x) = \delta(x - \epsilon_\beta^0 - \Sigma_\beta(x)) = \left(1 - \frac{\partial \Sigma_\beta}{\partial x}\bigg|_{\epsilon_\beta}\right)^{-1} \delta(x - \epsilon_\beta) \ , \tag{24}$$

where

$$\epsilon_\beta^0 = \tfrac{1}{2}\hbar\omega_c + \hbar^2(k_z - Q_z)^2/2m^*$$

and $\epsilon_\beta = \epsilon_\beta^0 + \Sigma_\beta(\epsilon_\beta)$ are the unperturbed and perturbed ground-state energies, respectively. Hence,

$$\Sigma_\alpha(E + i0) = \sum_{\vec{Q}} |v_{\beta\alpha}(\vec{Q})|^2 \left(1 - \frac{\partial \Sigma_\beta}{\partial x}\bigg|_{\epsilon_\beta}\right)^{-1} \times \left(\frac{1 - f(\epsilon_\beta) + N_Q}{E - \epsilon_\beta - \hbar\omega_Q \pm i0} + \frac{f(\epsilon_\beta) + N_Q}{E - \epsilon_\beta + \hbar\omega_Q \pm i0}\right) . \tag{25}$$

Except for the renormalization factor $(1 - (\partial\Sigma_\beta/\partial x)|_{\epsilon_\beta})^{-1}$ this is just a finite-temperature generalization of previous results.[24] Since $\Sigma_\beta$ is of order $\alpha_0$, the factor $[(1 - (\partial\Sigma_\beta/\partial x)|_{\epsilon_\beta})]^{-1}$ can be ignored, for it can alter the result only to higher orders of $\alpha_0$. The appearance of the perturbed polaron ground-state energy $\epsilon_\beta$ instead of $\epsilon_\beta^0$ is in agreement with Larsen *et al.*[2] $\Sigma_\alpha$ has been evaluated from (25) by Nakayama for an electron in an otherwise empty conduction band. His result is

$$\Sigma_\alpha(E + i0) = -\frac{\alpha_0(\hbar\omega_0)^{3/2}}{(E_c - E)^{1/2}} \int_0^\infty dx \, \frac{e^{-x^2} x^2 (x + \xi)}{(x + \xi)^2 + u^2} \quad \text{for } E < E_c, \tag{26}$$

and

$$\Sigma_\alpha(E + i0) = -\frac{i\alpha_0(\hbar\omega_0)^{3/2}}{2(E - E_c)^{1/2}} \int_0^\infty dx \, e^{-x^2} x^2 \times \frac{1}{x - i(\xi - u)} + \frac{1}{x - i(\xi + u)} \quad \text{if } E > E_c. \tag{27}$$

Here

$$\xi = (|E - E_c|/\hbar\omega_c)^{1/2} \ , \qquad u^2 = (\hbar^2 k_z^2/2m^*)(\hbar\omega_c)^{-1} ,$$

and $E_c = \epsilon_0 + \hbar\omega_0$, with $\epsilon_0$ the perturbed polaron ground state of an electron in state $n = 0$, $k_z = 0$. The resonance $\alpha_0|(E - E_c)/\hbar\omega_0|^{-1/2}$ is noteworthy and is responsible for the so-called pinning of the perturbed $n = 1$ level to $E_c$ in high magnetic fields[2] ($\omega_c > \omega_0$).

Thus far we have evaluated only the lowest-order skeleton-diagram (Fig. 2) contribution to the electron self-energy. It turns out, in fact, that the dominant contribution to $\Sigma_\alpha(\zeta_l)$ is given by (25). In the Appendix, estimates are given for the contributions of typical higher-order diagrams. Therein it is shown that the full EPI-vertex part $\Gamma_{\beta\alpha}(\vec{Q})$ can be replaced by the elementary EPI vertex $V_{\beta\alpha}(Q)$ and terms neglected are smaller by a factor of $\sim \alpha_0/|(E - E_c)/\hbar\omega_0|^{1/2}$. The EPI-vertex part $\Gamma_{\beta\alpha}(\vec{Q}, \zeta_l + \xi_m, \zeta_l)$ has a diagrammatic prescription illustrated in Fig. 3. It consists of the sum of all skeleton diagrams which have two external fermion lines, one incoming and one outgoing (labeled $\beta$ and $\alpha$, respectively) and an external phonon line. In the class of "ladder" skeleton diagrams, a propagation pair is introduced together with every internal phonon line. Under suitable conditions the denominators of the propagation pair can become simultaneously small and may introduce resonance stronger than $\alpha_0/|(E - E_c)/\hbar\omega_0|^{1/2}$ in higher-order diagrams. The purpose of the Appendix is to show that for $\alpha_0/|(E - E_c)/\hbar\omega_0| \lesssim 1$, all the higher-order vertex corrections are at least a factor $\alpha_0/|(E - E_c)/\hbar\omega_0|^{1/2}$ smaller than the elementary EPI vertex.

In their analysis of the perturbation series for the electron self-energy, Korovin and Pavlov have calculated $\Sigma_\alpha$ as in (25) but have used the unperturbed Green's function. Then they estimated two terms $\Sigma_{21}$ and $\Sigma_{22}$ (diagrammatically represented in Fig. 4) that appear in the next order of their perturbation scheme. The estimates are given as, in our notation,

$$\Sigma_{21} \simeq i\alpha_0^2(\hbar\omega_0)^{3/2}\hbar\omega_c/|E - E_c^0|^{3/2} , \tag{28}$$

$$\Sigma_{22} \simeq \alpha_0^2\hbar^2\omega_0\omega_c/|E - E_c^0| , \tag{29}$$

where $E_c^0 = \hbar\omega_0 + \frac{1}{2}\hbar\omega_c$. When $\alpha^0/|(E - E_c)/\hbar\omega_0| \sim 1$,

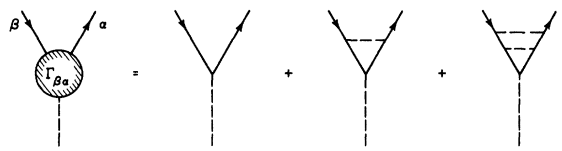


FIG. 3. The EPI-vertex part defined diagrammatically.

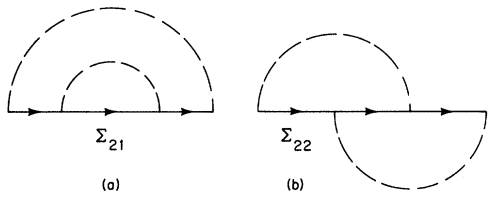


FIG. 4. Typical higher-order diagrams in Korovin and Pavlov's perturbation scheme.

clearly $\Sigma_{21}$ is not negligible in comparison with $\Sigma_1$. Indeed, higher-order multiphonon processes of the type $\Sigma_{21}$ are of the same order as $\Sigma_1$ and all should be included in their perturbation series. This complexity of the problem does not arise if we start out from (18), (19), and (20), and the approximation to it when the complete EPI-vertex part is replaced by the elementary EPI vertex. In fact these multiphonon terms can be formally generated from $\Sigma_\alpha(E)$ in (25) or (26) and (27) if we expand $\alpha_0/|(E-E_c)/\hbar\omega_0|^{1/2}$ as

$$\frac{\alpha_0}{|(E-E_c^0)/\hbar\omega_0|^{1/2}}\left(1+\frac{1}{2}\,\frac{\Sigma_0}{|(E-E_c^0)/\hbar\omega_0|}+\cdots\right);$$

$\Sigma_0$ is polaron self-energy for an electron in the $n=0$ state and is of order $\alpha\hbar\omega_0\omega_0$. The second term of this expansion can be identified with $\Sigma_{21}$ of Korovin and Pavlov. This expansion is invalid near the resonance when $\alpha_0/|(E-E_c^0)/\hbar\omega_0|$ is of $O(1)$ and the perturbation series has no meaning. From (29), the contribution $\Sigma_{22}$ of Fig. 4(b) is of an order $\alpha_0/|(E-E_c^0)/\hbar\omega_0|^{1/2}$ higher than $\Sigma_1$. This is in accordance with the general result of the Appendix which states that to within zeroth order in $\alpha_0/|(E-E_c)/\hbar\omega_0|^{1/2}$, the full EPI-vertex part can be replaced by the elementary EPI vertex.

To investigate the energy spectrum we require the spectral weight function $A_\alpha(E)=-(1/\pi)\mathrm{Im}G_\alpha(E)$ which is readily obtainable from (26) and (27). It has been shown by Nakayama[24] that $A_\alpha(E)$ is of the form

$$A_\alpha(E)=\left(1-\frac{\partial \mathrm{Re}\Sigma_\alpha}{\partial E}\bigg|_{E_\alpha^-}\right)^{-1}(E-E_\alpha^-)+\mathfrak{a}_\alpha(E)\,. \quad (30)$$

$E_\alpha^-(<E_c)$ is determined from the equation $E_\alpha^- - \epsilon_\alpha^0 - \mathrm{Re}\Sigma_\alpha(E_\alpha^-)=0$, and $\mathfrak{a}_\alpha(E)$ is a distorted Lorentzian function which vanishes identically for $E<E_c$. $E_\alpha^-$, which becomes pinned to $E_C$ when $\omega_C$ increases, represents the so-called lower branch, while $\mathfrak{a}_\alpha(E)$ corresponds to the upper branch and has been shown to have a peak above $E_c$ for any value of $\omega_c$.[24] The proof of the existence of the upper branch for any $\omega_c$ is due to Nakayama.

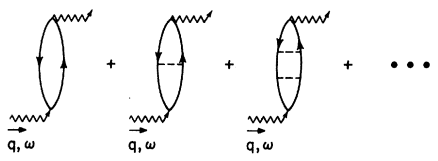


FIG. 5. Ladder-diagram contributions to the correlation function $R(\omega+i0)$.

## IV. SCATTERED-LIGHT SPECTRUM

In this section we shall evaluate the thermal correlation functions $\mathcal{F}_{\alpha\beta\delta\epsilon}(i\omega_n)$ and $\mathcal{R}(i\omega_n)$. The method of Luttinger and Ward[23] generalized by Holstein,[26] of introducing skeleton diagrams for $\mathcal{R}(i\omega_n)$ shall be used. The procedure amounts to summation over all distinct skeleton diagrams wherein each fermion or boson line is set equal to the exact propagator. The prescriptions for the construction and evaluation of correlation-function diagrams have been given by Holstein.[26] The rules given there are, for the most part, immediately applicable. The few changes are due to the one-electron basis set and the Landau states $\alpha\equiv|n_\alpha, k_y, k_z\rangle$ instead of plane waves. Thus the fermion line is $G_\alpha(\zeta_l)=[\zeta_l-\epsilon_\alpha^0-\Sigma_\alpha(\zeta_l)]^{-1}$. With each EPI vertex we now associate a factor $\mathcal{V}_{\beta\alpha}(\vec{\mathrm{Q}})$. For the incoming (outgoing) external-field vertex associate a factor $\gamma^*_{\alpha\beta}(\gamma_{\alpha\beta})$. Finally, to include el-el interaction we addend the rule so that for the incoming (outgoing) Coulomb-interaction vertex we associate a factor $m^*_{\alpha\beta}(m_{\alpha\beta})$, and for the Coulomb-interaction line a factor $v(\vec{\mathrm{q}})$.

Figure 5 represents some of the simplest skeleton diagrams that contribute to the correlation function $\mathcal{R}(\omega+i0)$. These are the so-called ladder diagrams which have significance for transport phenomena in metals. Nevertheless, we are interested only in resonant enhancement effects. Then it can be shown in a manner analogous to the Appendix that all the higher terms of the ladder-diagram series contribute at least an order $O(\alpha_0/|(E-E_c)/\hbar\omega_0|^{1/2})$ higher than the first member, and hence will be neglected. The el-el interaction shall now be in-

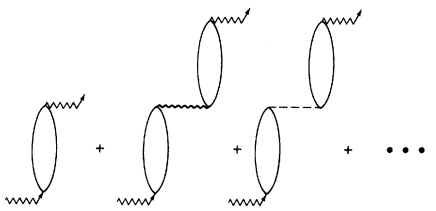

FIG. 6. RPA series of skeleton-diagram contributions to $R(\omega+i0)$. The wavy (dotted) line represents the el-el interaction $\mathcal{V}(\vec{\mathrm{q}})$ [phonon-induced el-el interaction $|\mathcal{V}(\vec{\mathrm{q}})|^2 \times D(\vec{\mathrm{q}}, i\omega_n)$].

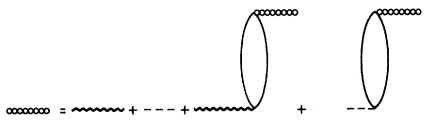

FIG. 7. Diagrammatic representation of the integral Eq. (33) for the effective el-el interaction $U_q(i\omega_n)$ (beaded line).

cluded in the random-phase approximation (RPA) only, which is presumably adequate in the long-wavelength limit $q \to 0$.[27] The RPA series of skeleton diagrams is shown in Fig. 6. This series of diagrams for $\mathcal{R}$ can be summed if we introduce an effective el-el interaction $U_{\vec{q}}(i\omega_n)$ schematically described as in Fig. 7. Then the skeleton diagrams that contribute to $\mathcal{R}$ are simply that of Fig. 8. We denote the term corresponding to the diagram shown in Fig. 9 as $Q_{\alpha\beta}(i\omega_n)$, whose functional form will be obtained explicitly in (39) below. If we apply our rules, then the effective el-el interaction $U_{\vec{q}}(i\omega_n)$ defined diagrammatically in Fig. 7 satisfies the algebraic relation

$$U_{\vec{q}}(i\omega_n) = \phi_{\vec{q}}(i\omega_n) + \phi_{\vec{q}}(i\omega_n)\, L_0(\vec{q}, i\omega_n)\, U_{\vec{q}}(i\omega_n) \tag{31}$$

or

$$U_{\vec{q}}(i\omega_n) = \phi_{\vec{q}}(i\omega_n)/\epsilon_T(\vec{q}, i\omega_n)\ . \tag{32}$$

We have here

$$L_0(\vec{q}, i\omega_n) \equiv \sum_{\alpha\beta} |m_{\alpha\beta}(\vec{q})|^2 Q_{\beta\alpha}(i\omega_n)\ . \tag{33}$$

The RPA polarization,

$$\phi_{\vec{q}}(i\omega_n) = v(\vec{q}) + |v(\vec{q})|^2 D(\vec{q}, i\omega_n)\ , \tag{34}$$

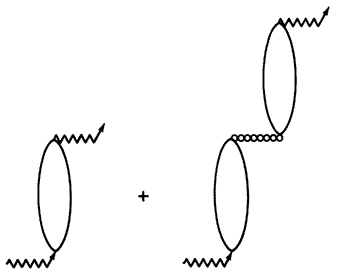

FIG. 8. Skeleton diagram for $R(i\omega_n)$ obtained via partial summation of the RPA series in Fig. 6.

with $D(\vec{q}, i\omega_n)$ the phonon propagator as in (19), is the bare effective el-el interaction, and

$$\epsilon_T(\vec{q}, i\omega_n) = 1 - \phi_{\vec{q}}(i\omega_n) L_0(\vec{q}, i\omega_n). \tag{35}$$

We readily obtain

$$U_{\vec{q}}(i\omega_n) = \frac{4\pi e^2}{q^2}\left(\epsilon_L(i\omega_n) + 1 - \frac{4\pi e^2}{q^2} L_0(\vec{q}, i\omega_n)\right)^{-1}\ , \tag{36}$$

where

$$\epsilon_L(\omega) = \epsilon_\infty\,[1 + (\omega_0^2 - \omega_t^2)/(\omega_t^2 - \omega^2)]$$

is the longitudinal dielectric constant of the polar lattice.

To evaluate the contribution to $\mathcal{R}(i\omega_n)$ from the two skeleton diagrams in Fig. 8, we apply the rules as mentioned earlier in this section, from which

$$\mathcal{R}(i\omega_n) = \sum_{\alpha\beta} |\gamma_{\alpha\beta}|^2 Q_{\beta\alpha}(i\omega_n) - U_q(i\omega_n) \times \left[\sum_{\alpha\beta} \gamma^*_{\alpha\beta} m_{\alpha\beta} Q_{\beta\alpha}(i\omega_n)\right]\left[\sum_{\alpha\beta} \gamma_{\alpha\beta} m^*_{\alpha\beta} Q_{\beta\alpha}(i\omega_n)\right] \tag{37}$$

and

$$Q_{\beta\alpha}(i\omega_n) = -k_B T \sum_{\zeta_l} \frac{1}{[\zeta_l - \epsilon^0_\beta - \Sigma_\beta(\zeta_l)][\zeta_l + i\hbar\omega_n - \epsilon_\alpha - \Sigma_\alpha(\zeta_l + i\hbar\omega_n)]} \tag{38}$$

The technique of evaluation of $Q_{\beta\alpha}(i\omega_n)$ is standard.[26] The $\zeta_l$ sum is converted to a contour integral in the complex $\zeta$ plane cut along the lines of discontinuity of the self-energy parts, i.e., the lines $\mathrm{Im}\zeta = 0$ and $\mathrm{Im}(\zeta + i\hbar\omega_n) = 0$. The contour integral is further reduced to integrals over a real variable, the continuation of $i\omega_n \to \omega + io$ is performed, and finally, one obtains

$$Q_{\beta\alpha}(\omega + io) = \iint d\epsilon\, d\epsilon'\, \frac{A_\alpha(\epsilon')A_\beta(\epsilon)}{\hbar\omega - (\epsilon' - \epsilon) + io} \times [f^-(\epsilon) - f^-(\epsilon')]. \tag{39}$$

We recall that $A_\alpha$ and $A_\beta$ are the spectral weight functions. Equations (9), (33), (36), (37), and (39) comprise the result of the light-scattering cross section. If we define

$$L_2 = \sum_{\alpha\beta} |\gamma_{\alpha\beta}|^2 Q_{\beta\alpha}(\omega + io),$$

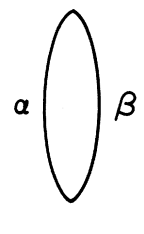


FIG. 9. Diagrammatic definition of $Q_{\alpha\beta}(i\omega_n)$.

$$L_1 = \sum_{\alpha\beta} \gamma_{\alpha\beta}\, m^*_{\alpha\beta}\, Q_{\beta\alpha}(\omega + i0),$$

$$\tilde{L}_1 = \sum_{\alpha\beta} \gamma^*_{\alpha\beta}\, m_{\alpha\beta}\, Q_{\beta\alpha}(\omega + i0),$$

$$L_0 = \sum_{\alpha\beta} |m_{\alpha\beta}|^2 Q_{\beta\alpha}(\omega + i0).$$

The result is

$$\frac{d^2\sigma}{d\omega d\Omega} = \frac{\omega_F}{\omega_I} \frac{1}{[1 - e^{-\hbar\omega/k_B T}]} \times \mathrm{Im}\left[L_2 + \frac{4\pi e^2}{q^2} \frac{L_1 \tilde{L}_1}{\epsilon_L(\omega) - (4\pi e^2/q^2) L_0}\right]. \quad (40)$$

Equation (40) has the same form as the expression for light scattering as given by Blum.[16] If we had been able to ignore the el-ph self-energy effects, then $A_\alpha(\epsilon') = \delta(\epsilon' - \epsilon^0_\alpha)$, $A_\beta = \delta(\epsilon - \epsilon^0_\beta)$, and $Q_{\beta\alpha}(\omega + i0)$ reduces simply to

$$[f(\epsilon^0_\alpha) - f(\epsilon^0_\beta)]/(\hbar\omega + \epsilon^0_\beta - \epsilon^0_\alpha + i0).$$

Then from (39) and (40) we can recapture the light-scattering cross-section formula as given in Eqs. (11–15) of Ref. 17. The resonant coupling of the Landau levels via LO-phonon emission can resonantly and quite drastically modify the nature of the single-particle states. As we have seen in Sec. III, all such relevant information is contained in the spectral weight functions $A_\alpha(\epsilon)$. Equation (39) shows how the resonant coupling could affect the scattered-light spectrum.

## V. LANDAU-RAMAN SCATTERING

In this section we shall examine the effect of the resonant coupling of Landau levels due to LO-phonon emission on the scattered-light spectrum. We shall confine our discussion mainly to the so-called Landau-Raman processes which correspond to excitation of electrons between Landau levels with the same spin quantum number and occur at $\omega$ near $N\omega_c$. Hence we shall ignore spin in the following considerations. To fix ideas we shall focus our attention on $d\sigma$ at $\omega$ near $2\omega_c$. The magnetic field strength and the electron concentration are such that only the lowest Landau level ($n = 0$) is occupied and $\omega_c$ is nearly $\omega_0$. The last condition implies that consecutive Landau levels could be resonantly coupled. One reason for the choice of the conditions $\omega = 2\omega_c$ is to avoid the observation of resonant coupling falling in the region of strong first-order scattering of optical phonons which could mask other effects.

Solution to the problem as defined will require knowledge of the nature of the $n = 2$ Landau level coupled to the $n = 1$ level via one-LO-phonon emission. We ignore the coupling of the $n = 2$ to the $n = 0$ level via two-LO-phonon emission because the effect of this is of an order $O(\alpha_0)$ higher. The study of this coupling is novel because the $n = 1$ level has already been drastically modified by phonon-emission processes as has been discussed amply in Sec. III. From (22) and (30) the self-energy part for an electron $|\alpha\rangle (\equiv |2, k_y, k_z\rangle)$ is

$$\Sigma_2(E + i0, k_z) = \sum_{\vec{Q}} |v_{\beta\alpha}(\vec{Q})|^2 \frac{Z_\beta}{E - E^-_\beta - \hbar\omega_Q + i0)} + \sum_{\vec{Q}} |v_{\beta\alpha}(Q)|^2 \int_{E_c}^{\infty} \frac{A_\beta(x)}{(E - x - \hbar\omega_Q + i0)} dx \; ; \quad (41)$$

here $|\beta\rangle \equiv |1, k_y - Q_x, k_z - Q_z\rangle$ and $Z_\beta$ denotes the renormalization

$$\left(1 - \frac{\partial\, \mathrm{Re}\Sigma_\beta}{\partial E}\bigg|_{E^-_\beta}\right)^{-1}.$$

$\Sigma_2$ in (41) can only be evaluated numerically. In the absence of specific experimental data to compare with we shall be satisfied with qualitative analytic behavior of $\Sigma_2$ as a function of magnetic field near the resonance region $\omega_c \approx \omega_0$.

When $\omega_c < \omega_0$ and off resonance, $E^-_\beta$ has a $(k_z - Q_z)$ dependence which goes approximately as $\hbar^2(k_z - Q_z)^2/2m^*$. The first term on the right-hand side of (41) dominates, and on evaluation yields a resonance of the form

$$\alpha_0(\hbar\omega_0)^{3/2}/|E - E'_c|^{1/2}$$

for either $E \lesssim E'_c [\equiv E^-_1(k_z = 0) + \hbar\omega_0]$. In the same manner as shown for $A_1(E, k_z)$ in Sec. III, if we evaluate the spectral weight function $A_2(E, k_z)$, we can verify the existence of an upper (lower) branch which asymptotically approaches $E'_c(\epsilon^0_\alpha)$ from above (below) for decreasing magnetic field. Notice that for $E < E'_c$, $\Sigma_2(E, k_z)$ is real. Hence the aforementioned lower branch is a $\delta$ function and the upper branch a distorted Lorentzian whose peak defines the branch itself. The second term in (41), though small in the asymptotic region $\omega_c < \omega_0$, can give rise to yet another upper branch which approaches $E''_c [\equiv \epsilon_0(k_z = 0) + 2\hbar\omega_0]$ when $\omega_c$ decreases. This can be seen if we recall $A_\beta(x)$ defines the upper branch of state $|\beta\rangle$ which approaches asymptotically $E_c$ and whose dependence on $k_z - Q_z$ is weaker as $\omega_c$ decreases. This band-flattening effect enhances the divergence of the density of final states leading to a resonance when $E$ is near $E''_c$. The existence of such an upper branch is then clear.

If $\omega_c > \omega_0$, the dependence of $E^-_\beta$ on $k_z - Q_z$ becomes weaker as $\omega_c$ increases. Thus the band flattens and enhances the divergence of the final-states

density and the resonance near $E_c'$. In spite of the fact that $Z_\beta$ decreases, such a resonance will give rise to a lower branch pinned to $E_c'$ as $\omega_c$ increases. Note that as $\omega_c$ increases, $E_c' \to E_c''$. Further we examine the asymptotic behavior ($\omega_c > \omega_0$) of the second term in (41). $\alpha_1(x, k_z - Q_z)$ approaches the form of a Lorentzian whose maximum tends to have the $\hbar^2(k_z - Q_z)^2/2m^*$ dependence.[24] Whence the second term contributes a convolution of resonances $\alpha_0(\hbar\omega_0)^{3/2}/|E-x|^{1/2}$ with $\alpha_1(x)$. Let $E_c'''$ be equal to $\epsilon_1(k_z=0)+\hbar\omega_0$. It follows that a broadened lower (upper) branch which approaches $E_c'''(\epsilon_\alpha^0)$ from above, exists. Since $E_c''' > E_c'$ for $\omega_c > \omega_0$, the first term of (41) contributes an imaginary part to the self-energy and further broadens the lower branch.

Results obtained are qualitatively illustrated in Fig. 10. Described in terms of the spectral weight function, the lowest branch (I) contributes a $\delta$ function

$$\left(1 - \frac{\partial\, \mathrm{Re}\Sigma_2(E, k_z)}{\partial E}\bigg|_{E_2^-(k_z)}\right)^{-1} \delta(E - E_2^-(k_z))$$

to $A_2(E_1, k_z)$. Here $E_2^-(k_z) < E_c''$ satisfies the equation $E - \epsilon_\alpha^0 - \Sigma_2(E, k_z) = 0$. The other lower branch (II) and the upper branch (III) contribute a term $\alpha_2(E, k_z)$ which has two peaks whose maxima as a function of $\omega_c$ are what we have called branches II and III. Explicitly,

$$A_2(E, k_z) = Z_{2,k_z}\,\delta[E - E_2^-(k_z)] + \alpha_2(E, k_z). \tag{42}$$

We shall proceed to calculate the cross section for scattering near $\omega = 2\omega_c$ that involves single-particle excitation from $\beta = |0, k_y, k_z\rangle$ to $\alpha = |2, k_y + q_y, k_z + q_z\rangle$. Integrate $Q_{\beta\alpha}(\omega + i0)$ in (39) over $k_y$ and denote the result by $Q_{k_z}(\omega + i0)$; then

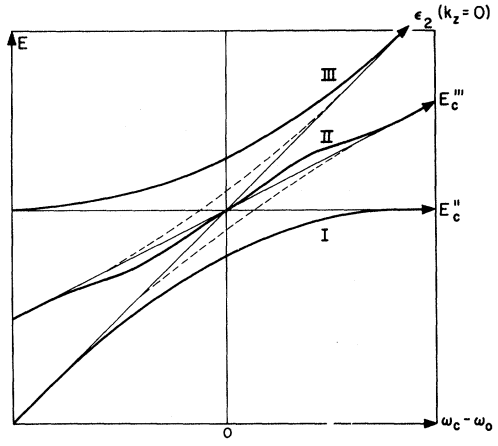


FIG. 10. The energy spectrum of an electron in state $|\alpha\rangle \equiv |2, k_y, k_z\rangle$ (schematic). See text for explanation.

$$Q_{k_z}(\omega + i0) = \int d\epsilon\, \frac{\rho(\epsilon_\beta) - \rho(\epsilon)}{\hbar\omega + \epsilon_\beta - \epsilon + i0} \times [Z_{2,k_z}\,\delta(\epsilon - E_2^-(k_z)) + \alpha_2(\epsilon, k_z)] \tag{43}$$

and

$$L_2 = \int (dk_z/2\pi)\, |\gamma(0, k_z; 2, k_z + q_z)|^2\, Q_{k_z}(\omega + i0), \tag{44}$$

$$L_1 = \int (dk_z/2\pi)\, \gamma(0, k_z; 2, k_z + q_z) m_{\alpha\beta}^*\, Q_{k_z}(\omega + i0), \tag{45}$$

$$\tilde{L}_1 = \int (dk_z/2\pi)\, \gamma^*(0, k_z; 2, k_z + q_z) m_{\alpha\beta}\, Q_{k_z}(\omega + i0), \tag{46}$$

$$L_0 = \int (dk_z/2\pi)\, |m_{\alpha\beta}|^2\, Q_{k_z}(\omega + i0), \tag{47}$$

$$\rho(\epsilon) = \int (dk_y/2\pi) f(\epsilon). \tag{48}$$

### A. Scattering Parallel to Magnetic Field

The matrix element $m_{\alpha\beta}$ vanishes and the $U_q L_1 \tilde{L}_1$ term in the cross section gives no contribution, thus

$$\frac{d^2\sigma}{d\omega d\Omega} = \frac{\hbar\omega_F}{\pi\omega_I}\, \frac{1}{1 - e^{-\hbar\omega/k_B T}}\, \mathrm{Im} L_2 \tag{49}$$

and

$$\mathrm{Im} L_2 = \int (dk_z/2\pi)\, |\gamma(0, k_z; 2, k_z + q_z)|^2 \times [\rho(\epsilon_\beta) - \rho(\epsilon_\beta + \hbar\omega)] \times \pi[Z_{2,k_z+q_z}\,\delta(\epsilon_\beta + \omega - E_{2,k_z+q_z}^-) + \alpha_2(\epsilon_\beta + \omega, k_z + q_z)]. \tag{50}$$

We recall that both the el-el and el-ph interactions can affect the matrix elements $\gamma_{\alpha\beta}$. Harper[19] has indeed shown that the modification of $\gamma_{\alpha\beta}$ due to the resonant el-ph coupling can contribute an additional scattering mechanism which he estimated to be of the order of $\alpha_0^2\,\sigma_T^*$. However, in III–V semiconductors of the InSb-type interband transitions contribute a significant cross section which has been estimated to be[17] $\sigma_{2\omega_c} \sim (\hbar\omega_c/E_g)^2\sigma_T^*$. This is two orders of magnitude larger than the resonant-coupling-induced cross section of Harper for InSb at fields near 30 kG. This fact serves to justify our approximation on $\gamma_{\alpha\beta}$ and illustrates the difference between Harper's problem and ours. The effect on the cross section due to the resonant coupling via LO phonons is contained in (50). For 10.6-$\mu$ laser light, $q_z$ ($< 10^4$ cm$^{-1}$) is negligible. Integration of $dk_z$ introduces the singularity in the state density at $k_z = 0$. The scattered-light spectrum

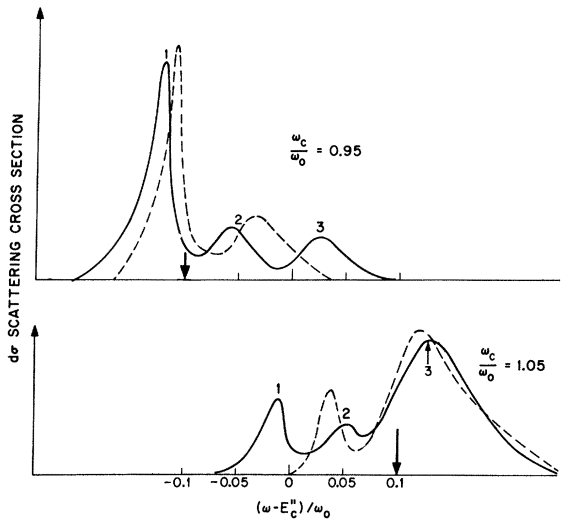


FIG. 11. The spectrum of scattered light as a function of $\omega$ (schematic) for two values of $\omega_c/\omega_0$. Arrow indicates the position of the unperturbed $|2, k_y, k_z\rangle$ state for small $k_z$.

from (50) for several magnetic field strengths are schematically represented in Fig. 11. Three peaks are expected to consist of the scattered-light spectrum for any magnetic field strength near resonance, though their relative strengths can vary. These peaks labeled 1, 2, and 3 correspond to scattering with electron transitions to branches I, II, and III, respectively. If $\omega_c/\omega_0 < 1$ and for decreasing field peaks, 2 and 3 diminish in strength and 2(3) is approaching $E_c'(E_c'')$ and remains above it. On the other hand, if $\omega_c/\omega_0 > 1$ and for increasing field peak, 3 grows in strength and tends to the unperturbed $|2, k_z = 0\rangle$-state energy, while 2(1) is approaching $E_c''(E_c')$ from below and both are diminishing in strength.

### B. Scattering Perpendicular to the Magnetic Field

Consider perpendicular scattering with $q_z = 0$. The cross section for Landau-Raman scattering is screened by the Coulomb interactions as will be shown by the example that involves transitions from $|\beta\rangle \equiv |0, k_y, k_z\rangle$ to $|\alpha\rangle \equiv |2, k_y + q_y, k_z\rangle$. We shall take over the notations as defined in (43)–(48) but with $q_z = 0$. Decompose into real and imaginary parts, so that

$$Q_{k_z}(\omega + i0) = P\int d\epsilon \frac{\rho(\epsilon_\beta) - \rho(\epsilon)}{\hbar\omega + \epsilon_\beta - \epsilon} A_2(\epsilon_\beta + \hbar\omega, k_z) - i\pi[\rho(\epsilon_\beta) - \rho(\epsilon_\beta + \hbar\omega)] A_2(\epsilon_\beta + \hbar\omega, k_z). \quad (51)$$

Inserting this expression into (44)–(47), each of the $L$ functions can be separated into two terms, e.g., $L_2 = \mathfrak{L}_2 + i l_2$, etc. $\mathfrak{L}(l)$ comes from the real (imaginary) part of $Q_{k_z}$. For example,

$$l_1 = -\int (dk_z/2\pi)\gamma_{\alpha\beta} m_{\alpha\beta}^* \pi[\rho(\epsilon_\beta) - \rho(\epsilon_\beta + \hbar\omega)] \times A_2(\epsilon_\beta + \hbar\omega).$$

On computing the cross section we obtain

$$\frac{d^2\sigma}{d\omega d\Omega} = \frac{\hbar\omega_F}{\omega_I} \frac{1}{1 - e^{-\hbar\omega/kT}} \mathrm{Im}[L_2 - U_{\tilde{q}}(\omega) L_1 \tilde{L}_1] \quad (52)$$

and

$$\mathrm{Im}(L_2 - U_{\tilde{q}}(\omega) L_1 L_1) = l_2 - (\mathfrak{L}_1 \tilde{l}_1 + \tilde{\mathfrak{L}}_1 l_1)/\mathfrak{L}_0 - \mathfrak{L}_1 \tilde{\mathfrak{L}}_1 l_0/\mathfrak{L}_0^2. \quad (53)$$

Equation (53) gives the scattered-light spectrum in terms of the spectral weight function $A_2(E, k_z)$. The first term on the right is the one-electron contribution which is screened by the last two terms. For a realistic III-V-semiconductor plasma, the screening is only partial. In fact it has been shown[17] that if the $k_z$ dependence of $\gamma$ is accounted for, the cross section per particle is $\sigma_{2\omega_c} = 0[\frac{2}{15}\sigma_T^*(E_F/E_g)^2]$. Here $E_F$ is the Fermi energy referred to the band minimum of the lowest Landau level. Though (53) is more complicated than the expression for scattering parallel to the magnetic field, resonant el-ph coupling will have the same effect on the spectrum as qualitatively described in Fig. 11.

The $n = 2$ level scheme and scattered-light spectrum, as described, apply to rather pure samples only. For InSb, by rather pure samples we mean ones with electron concentration $N \approx 10^{14}$ cm$^{-3}$, such as are often used in cyclotron resonance experiments.[1] To date, light-scattering experiments from semiconductor electron plasma are usually done for $N \gtrsim 10^{15}$ cm$^{-1}$. At values of the magnetic field such that only the zeroth Landau level is occupied and for $N$ sufficiently large when $E_F - \mathcal{E}_0(k_z = 0) \gg \alpha_0 \hbar\omega_0$, pinning to $E_c''$ disappears and the three branches I, II, and III collapse to the two shown as the broken curves in Fig. 10. The corresponding cross section for values of the magnetic field near the resonance has now only two peaks shown as the broken curves in Fig. 11. The strength of the scattering cross section moves from the lower branch to the upper one with increase of $\omega_c$.

## VI. MAGNETOPLASMA AND COUPLED LO-PHONON-MAGNETOPLASMA MODE

We shall briefly consider here the possibility of observing resonance-enhanced polaron effects similar to that which occurs for single-particle excitations, in the magnetoplasma waves[27] or the coupled LO-phonon–magnetoplasma mode.[28] There

has been some experimental interest[29] to search for these effects. The purpose of the following is to demonstrate such effects are nonexistent.

The linear response of the electron-lattice system is described by the dielectric function given via (36). To arrive at the coupled magnetoplasma–LO-phonon modes, we look for poles in the response function or zeros of the dielectric function. From (36), these normal modes $\omega(q)$ satisfy the equation

$$\epsilon_L(\omega) + 1 - (4\pi e^2/q^2)\, L_0(q, \omega) = 0. \tag{54}$$

If we neglect, at the moment, the resonant coupling of Landau levels, evaluating $L_0(q, \omega)$ in the long-wavelength limit $q \to 0$, we find that[28]

$$(4\pi e^2/q^2)\, L_0(q, \omega) = \omega_p^2 \sin^2\theta/(\omega^2 - \omega_c^2) + (\omega_p^2 \cos^2\theta)/\omega^2, \tag{55}$$

where $\omega_p = 4\pi Ne^2/m^*$ is the plasma frequency and $\theta$ is the angle between $\vec{q}$ and $\vec{H}$. For $\vec{q} \perp \vec{H}$, substituting (55) into (54) and solving for the normal modes, we rederive the expressions as were given by Kaplan *et al.*[30]

From this dielectric formulation of the coupled modes it is clear that any effect due to resonant coupling of Landau levels via LO-phonon emission occurs through modification of

$$L_0(\vec{q}, \omega) = \sum_{\alpha\beta} |m_{\alpha\beta}(\vec{q})|^2 Q_{\beta\alpha}(\vec{q}, \omega).$$

In the limit $q \to 0$, $|m_{\alpha\beta}(\vec{q})|^2$ is of order $q_\perp^{2|n_\alpha - n_\beta|}$ and since we require only all the terms of order $q^2$ in $L_0$, we need only consider terms in the summation over $\alpha$ and $\beta$ with $n_\alpha = n_\beta$, $n_\beta \pm 1$. The resonant coupling of Landau levels alters the spectral weight functions in (39) for $Q_{\beta\alpha}(q, \omega)$. Assume $|\alpha\rangle$ is resonating with $|\beta\rangle$ plus one LO phonon, and $n_\alpha = n_\beta + 1$. From (25), the $[1 - f(\epsilon_\beta)]$ factor in the phonon-emission term implies that resonance of the form $\alpha_0/|E - E_c|^{1/2}$ exists only if the $n_\beta$ level is sparingly occupied such that $E_F - \epsilon_{n_\beta}(k_z = 0)$ (the Fermi energy measured from the $n_\beta$-level minimum) is less than $\alpha_0 \hbar\omega_c$. Nevertheless, even when the last condition prevails the combination of Fermi factors in (43) implies the contribution to $L_0(q, \omega)$ is negligibly small. The arguments here preclude the observation of resonant coupling of Landau-level effects in the coupled magnetoplasmon-LO modes or the magnetoplasma waves.

## VII. DISCUSSION

We have thus extended the theory of light scattering from a semiconductor plasma to include el-ph interactions. In the course of the discussion we have shown that resonant coupling of Landau levels via LO phonons can cause magnetic-field-dependent structures in the Landau-Raman scattering spectrum. In our discussion we have focused our attention on the $n = 2$ level. Under the conditions as states in V, its level scheme has features different from the $n = 1$ level (see Fig. 10). In addition to Raman scattering, infrared cyclotron resonance experiments should also be able to reveal its structure. Preliminary experimental results[31] in InSb have confirmed these features. Throughout the discussion we have neglected the complexity of the magnetic energy levels in the conduction band of InSb-type semiconductors.[32,33] With inclusion of such band effects, the cyclotron resonance frequency at a given value of magnetic field will depend upon $n$, the Landau-level quantum number. The effect of this is to limit the validity of our analysis to energies $E$ outside bands of width $\hbar\Delta\omega_c$ centered around the pinning lines $E_c''$ and $E_c'''$. Here $\Delta\omega_c$ is the difference between the two cyclotron frequencies at a magnetic field near resonance. Otherwise the results we have obtained for the energy spectrum of the $n = 2$ level remain unaltered. For InSb, $\Delta\omega_c$ can be estimated from the magnetic energy levels at $k_z = 0$ deduced from experiments.[34] At $H \approx 30$ kG, $\hbar\Delta\omega_c$ is about 1 meV. Moreover, the density of states near the bottom of the conduction band can be expected to depart from simple parabolic-band behavior, principally because of interactions between the conduction band and other nearby bands.[33] However, any modifications on the predicted magnetic-field-dependent structures in the scattered-light spectrum due to band nonparabolicity is not important as can be seen from a recent calculation by Johnson and Dickey.[35] They have considered the variations of infrared cyclotron resonance and the density of states near the conduction-band edges of InSb. Their calculated cyclotron resonance joint density of states, as obtained from dispersion relations based upon $k \cdot p$ interactions with nearby bands and parameters determined by experiment, is broadened by less than 0.5 meV. Finally, since only phonons near the zone center are involved in the polaron self-energy of a semiconductor plasma under a strong magnetic field, the dispersion of LO phonons can also be ignored.

## ACKNOWLEDGMENTS

I should like to thank D. M. Larsen, F. A. Blum, and E. J. Johnson for many valuable discussions on these problems. I also wish to thank R. W. Davies, M. M. Litvak, A. L. McWhorter, and H. J. Zeiger for a critical reading of the manuscript.

## APPENDIX

In this Appendix the contributions of some typical

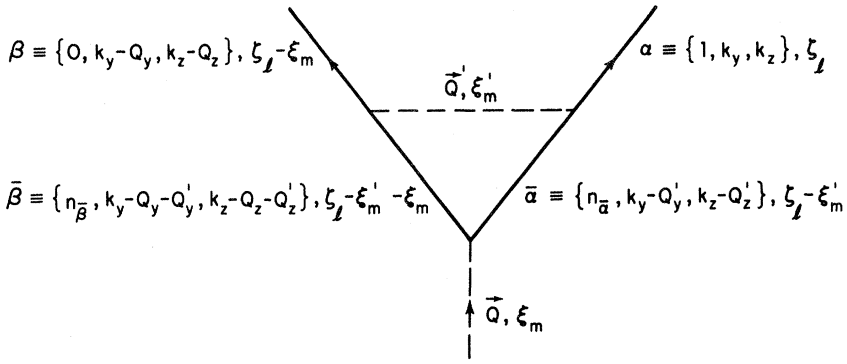


FIG. 12. Lowest-order skeleton diagram for the EPI-vertex part.

higher-order diagrams to the el-ph interaction-vertex part will be considered. We shall find that these contributions are smaller than the bare el-ph vertex part at least by an order $\alpha_0/|(E-E_c)/\hbar\omega_0|^{1/2}$, thereby justifying their neglect. The vertex part has been defined by the diagrammatic prescription illustrated in Fig. 3; explicitly one has

$$\Gamma_{\alpha\beta}(\vec{Q}, \zeta_l - \xi_m, \zeta_l) = v_{\alpha\beta}(\vec{Q}) + v_{\alpha\beta}^{(1)}(\vec{Q}, \zeta_l - \xi_m, \zeta_l) + v_{\alpha\beta}^{(2)}(\vec{Q}, \zeta_l - \xi_m, \zeta_l) + \cdots . \tag{A1}$$

$v_{\alpha\beta}^{(1)}$ is the lowest-order correction and is fully illustrated in Fig. 12. According to the rules of evaluating skeleton diagrams,[25]

$$v_{\alpha\beta}^{(1)}(\vec{Q}, \zeta_l - \xi_m, \zeta_l) = k_B T \sum_{\vec{Q}', n_{\bar{\alpha}}, n_{\bar{\beta}}, \zeta_{l'}, \pm} \frac{v_{\alpha\bar{\alpha}}(Q) v_{\bar{\beta}\bar{\beta}}(Q') v_{\bar{\alpha}\bar{\beta}}(Q)}{[\hbar\omega_{Q'} \pm (\zeta_l - \zeta_{l'} - \xi_m)][\zeta_{l'} - \epsilon_{\bar{\beta}} - \sum_{\bar{\beta}}(\zeta_{l'})][\zeta_{l'} + \xi_m - \epsilon_{\bar{\alpha}} - \epsilon_{\bar{\alpha}}(\zeta_{l'} + \xi_m)]} \cdot \tag{A2}$$

In the sum over $n_{\bar{\alpha}}$ and $n_{\bar{\beta}}$ we shall isolate our attention to only the summand with $n_{\bar{\alpha}} = 0$ and $n_{\bar{\beta}} = 1$. The summation over $\zeta_{l'}$ is converted to an integration over $\zeta_{l'}$, analogous to that leading from (20) to (23). The $\vec{Q}'$ sum is converted to an integral over $Q_\perp'$, $Q_z'$ and $\phi'$ (the azimuthal angle of $\vec{Q}'$).[21] Further, to obtain an estimate of $V_{\alpha\beta}^{(1)}$ it is legitimate to replace the electron propagators contained in (A2) by free propagators. We arrive at the estimate

$$\frac{v_{\alpha\beta}^{(1)}(\vec{Q}, \zeta_l - \xi_m, \zeta_l)}{v_{\alpha\beta}(\vec{Q})} = \int\int dQ_z' dQ_\perp' Q_\perp'^2 |v_{\bar{\alpha}\bar{\beta}}(\vec{Q}')|^2 J_2\left(\frac{\hbar Q_\perp Q_\perp'}{m^* \omega_c}\right) \times \sum_{\pm} \left( \frac{f^{(\mp)}(\epsilon_{\bar{\beta}})}{\hbar\omega_{Q'} \pm (\zeta_l - \xi_m - \epsilon_{\bar{\beta}})} - \frac{f^{(\mp)}(\epsilon_{\bar{\alpha}})}{\hbar\omega_{Q'} \pm (\zeta_l - \epsilon_{\bar{\alpha}})} \right) \frac{1}{\epsilon_{\bar{\beta}} + \xi_m - \epsilon_{\bar{\alpha}}} . \tag{A3}$$

Here $J_2$ denotes the Bessel function and $f^{(\mp)}$ the Fermi occupancy (vacancy) function, as defined before. The term in (A3) that contains the factor $f^{(\mp)}(\epsilon_{\bar{\alpha}})/[\zeta_l - \epsilon_{\bar{\alpha}} - \hbar\omega_{Q'}]$ will lead to a resonant contribution. In fact, from (17a), explicitly, it is

$$\int\int dQ_z' dQ_\perp' \frac{\hbar Q_\perp'^3}{2m^*\omega_c} |v_{\vec{Q}'}|^2 e^{-\hbar Q_\perp'^2/2m^*\omega_c} J_2\left(\frac{\hbar Q_\perp' Q_\perp}{m^*\omega_c}\right) \frac{f^+(\epsilon_{\bar{\alpha}})}{\zeta_l - \epsilon_0(k_z = 0) - (\hbar^2/2m^*)(k_z - Q_z)^2 - \hbar\omega_{Q'}} \frac{1}{\epsilon_{\bar{\beta}} + \xi_m - \epsilon_{\bar{\alpha}}} . \tag{A4}$$

Integration over $dQ_z'$ contributes a resonance of order

$$\alpha_0/|(\zeta_l - E_c)/\hbar\omega_0|^{1/2} .$$

We have also examined higher-order vertex parts $v_{\alpha\beta}^{(2)}$, etc. Although the addition of an extra phonon line leads to the appearance of an extra propagator pair which could yield a resonance, yet we can show for all $n \geq 1$, $v_{\alpha\beta}^{(n)}$ is at least of order $\alpha_0^{3/2}/|(E-E_c)/\hbar\omega_0|^{1/2}$. This justifies the replacement of the full el-ph vertex part $\Gamma_{\alpha\beta}$ by the bare vertex $v_{\alpha\beta}(Q)$.

*Work sponsored by the Department of the Air Force.

[1]E. J. Johnson and D. M. Larsen, Phys. Rev. Letters 16, 655 (1966).
[2]D. M. Larsen and E. J. Johnson, J. Phys. Soc. Japan

Suppl. 21, 433 (1966).
[3]D. H. Dickey and D. M. Larsen, Phys. Rev. Letters 20, 65 (1968).
[4]R. Kaplan and R. F. Wallis, Phys. Rev. Letters 20, 1499 (1968).
[5]D. H. Dickey, E. J. Johnson, and D. M. Larsen, Phys. Rev. Letters 18, 599 (1967).
[6]C. J. Summers, P. G. Harper, and S. D. Smith, Solid State Commun. 5, 615 (1967).
[7]C. J. Summers, R. B. Dennis, B. S. Wherrett, P. G. Harper, and S. D. Smith, Phys. Rev. 170, 755 (1968).
[8]J. Waldman, D. M. Larsen, P. E. Tannenwald, C. C. Bradley, D. R. Cohn, and B. Lax, Phys. Rev. Letters 23, 1033 (1969).
[9]B. D. McCombe and R. Kaplan, Phys. Rev. Letters 21, 756 (1968).
[10]*Light Scattering Spectra of Solids*, edited by G. B. Wright, (Springer-Verlag, New York, 1969).
[11]P. A. Wolff, Phys. Rev. Letters 16, 225 (1966).
[12]P. M. Platzman, P. A. Wolff, and N. Tzoar, Phys. Rev. 174, 489 (1968).
[13]D. C. Hamilton and A. L. McWhorter, Phys. Rev. Letters 21, 309 (1968).
[14]P. A. Wolff, Phys. Rev. 171, 436 (1968).
[15]A. L. McWhorter and P. N. Argyres, Phys. Rev. Letters 21, 325 (1968).
[16]P. M. Platzman and N. Tzoar, Phys. Rev. 182, 510 (1969).
[17]F. A. Blum, Phys. Rev. B 1, 1125 (1970).
[18]H. Frohlich, *Polarons and Excitons*, edited by C. G. Kuper and G. D. Whitfield (Oliver and Boyd, Edinburgh, 1963), p. 1.
[19]P. G. Harper, Phys. Rev. 178, 1229 (1969).
[20]A. A. Abrikosov, P. P. Gor'kov, and I. E. Dzyaloshinski, *Methods of Quantum Field Theory in Statistical Physics* (Prentice-Hall, Englewood Cliffs, N. J., 1963).
[21]T. M. Rice, Ann. Phys. (N. Y.) 31, 100 (1965).
[22]H. Scher and T. Holstein, Phys. Rev. 148, 598 (1966).
[23]J. M. Luttinger and J. C. Ward, Phys. Rev. 118, 1417 (1960).
[24]L. I. Korovin and S. T. Pavlov, Zh. Eksperim. i Teor. Fiz. 53, 1708 (1967) [Soviet Phys. JETP 26, 979 (1968)].
[25]M. Nakayama, J. Phys. Soc. Japan 27, 636 (1969).
[26]T. Holstein, Ann. Phys. (N. Y.) 29, 410 (1964).
[27]P. Nozières and D. Pines, Phys. Rev. 113, 1254 (1959).
[28]N. D. Mermin and E. Canel, Ann. Phys. (Paris) 25, 247 (1964).
[29]S. Iwasa, Y. Sawada, E. Burstein, and E. D. Palik, J. Phys. Soc. Japan Suppl. 21, 742 (1966).
[30]R. Kaplan, E. D. Palik, R. F. Wallis, S. Iwasa, E. Burstein, and Y. Sawada, Phys. Rev. Letters 18, 159 (1967).
[31]E. J. Johnson and K. L. Ngai (unpublished).
[32]R. Bowers and Y. Yafet, Phys. Rev. 115, 1165 (1959).
[33]B. Lax, J. G. Mavroides, H. J. Zeiger, and R. J. Keyes, Phys. Rev. 122, 31 (1961).
[34]E. J. Johnson and D. H. Dickey, Phys. Rev. B 1, 2676 (1970).
[35]E. J. Johnson and D. H. Dickey, in Proceedings of the Electronic Density of States Conference, Natl. Bur. Std. (U. S.), 1970 (unpublished).

PHYSICAL REVIEW B VOLUME 3, NUMBER 4 15 FEBRUARY 1971

# Piezoreflectivity of Gallium Arsenide†

J. E. Wells and P. Handler

*Department of Physics and Materials Research Laboratory, University of Illinois, Urbana, Illinois* 61801

(Received 24 February 1970)

The response of the reflectivity spectrum of single-crystal gallium arsenide to uniaxial stress in the [001] and [111] directions was determined. Interband transitions were detected at 1.425 ±0.015, 1.76 ±0.02, 2.89, 3.12, and 4.5 eV. The direct edge at Γ is found to have a deformation potential ratio $d/b \simeq 3.2$, using a stress-optical response model based on the Pikus – Bir Hamiltonian. The 2.89- and 3.12-eV spin-orbit-split transitions exhibit modulated reflectivity line shapes expected of Λ symmetry. Comparison is made with the stress-modulated response of a symmetry-related transition in germanium. The deformation-potential ratios $D_1^5/D_1^1 = -0.55$ ±0.03, $D_3^5/D_3^3 = 0.77$ ±0.03 have been derived. Comparison of the hydrostatic component of the perturbation with the energy derivative of the unmodulated reflectivity spectrum shows good agreement with a rigid-shift model. Finally, the 4.5-eV transition has shown a response to the stress perturbation indicative of a Δ symmetry.

## I. INTRODUCTION

The band structure of gallium arsenide has been investigated in recent years by a number of differential optical-reflection techniques. Perturbations as electric fields,[1,2] temperature,[3] stress,[4] or combinations of these effects[5] have been used to lift degeneracies and shift the energy bands in an attempt to obtain modulated reflectivity line shapes characteristic of the band symmetry.

Stress, as a perturbation, is, in many respects, the ideal approach to band-structure analysis. The band symmetries are easily traced from the undeformed to the deformed structure by elementary